DALTON
FULL PAPER

Comparison of the high-pressure and low-temperature structures of sulfuric acid

David R. Allan,[a] Stewart J. Clark,[b] Alice Dawson,[c] Pamela A. McGregor[a] and Simon Parsons[c]

[a] *Department of Physics and Astronomy, The University of Edinburgh, Mayfield Road, Edinburgh, UK EH9 3JZ*
[b] *Department of Physics, Durham University, Science Laboratories, South Road, Durham, UK DH1 3LE*
[c] *Department of Chemistry, The University of Edinburgh, West Mains Road, Edinburgh, UK EH9 3JJ*

Received 16th October 2001, Accepted 6th February 2002
First published as an Advance Article on the web 13th March 2002

We have determined the high-pressure crystal-structure of sulfuric acid, including the positions of the hydrogen atoms, using a combination of single-crystal X-ray diffraction techniques and *ab initio* density functional calculations. Just above the onset of crystallization, at 0.7 GPa, we find that a previously unobserved monoclinic structure, with $P2_1/c$ symmetry, is formed which is characterised by $SO_2(OH)_2$ tetrahedra interconnected by hydrogen bonds. In contrast to the low-temperature $C2/c$ phase, the tetrahedra in the high-pressure crystal structure are no longer arranged in $R_4^4(16)$ hydrogen-bonded layers but, instead, they form chains where the hydrogen bonding adopts a $R_3^3(12)$ arrangement. A series of *ab initio* calculations indicates that this rearrangement of the molecules results in a relatively small reduction in the enthalpy (13.603 kJ mol^{-1}) for the $P2_1/c$ structure at 0.7 GPa.

Introduction

Sulfuric acid (H_2SO_4) is a ubiquitous chemical reagent and is used for a very wide range of synthetic processes within both the academic and industrial disciplines. It is the largest volume chemical commodity and it can be used in the production of phosphate fertilizers, inorganic pigments, as a leaching agent in metal extraction and a variety of other economically important applications. Sulfuric acid can be readily co-crystallized with other molecular species: for example, the H_2SO_4–H_2O system has six intermediate compounds, $H_2SO_4{\cdot}nH_2O$ with n = 1, 2, 3, 4, 6.5, 8;[1] and simple salts can be produced with other acids, such as acetic acid (forming $CH_3C(OH)_2^+{\cdot}HSO_4^-$).[2,3] Anhydrous sulfuric acid crystallizes into a monoclinic crystal structure, with $C2/c$ symmetry, at approximately 10 °C. The structure is composed of layers of $SO_2(OH)_2$ tetrahedra connected *via* hydrogen bonds which, in turn, form four-fold, $R_4^4(16)$, nets as a result of the pairs of acceptor and donor oxygen atoms of the H_2SO_4 molecule.[4] Due to the nature of the hydrogen-bond network in the layers, the $C2/c$ crystal structure of H_2SO_4 has been regarded as a two-dimensional version of the well known KH_2PO_4 (KDP) structure, and it was considered possible that hydrogen-bond ordering transitions could occur at low temperature. However, neutron powder-diffraction studies of the structure revealed that the hydrogen-bond networks were ordered over a range of temperatures from near to the melting point down to the 10 K limit of the studies.[5] In KDP the hydrogen-ordering transition temperature (T_c) can be altered with the application of high-pressure as the hydrogen–hydrogen site separation (δ) is directly coupled to the distance between the acceptor and donor oxygens ($2R$). With increasing pressure $2R$ decreases with an accompanying decrease in both δ and T_c.[6,7] Although it would be anticipated that H_2SO_4 would adopt a similar behaviour and high-pressure would induce disorder, no high-pressure study of sulfuric acid appears to have been conducted to date.

We have recently determined the high-pressure crystal structures of the first three members of the monocarboxylic series—formic acid, acetic acid and propionic acid—and we have found that they all exhibit new structural phases at pressures just in excess of that required for crystallization.[8–10] All three of the organic acid systems investigated so far, therefore, have shown that profound structural modification can be induced by the application of fairly modest pressures (*i.e.* pressures in the 0.2 to 1.0 GPa regime) and it can be expected that the mineral acids, for example nitric acid, hydrochloric acid and sulfuric acid should exhibit equally rich high-pressure structural behaviour. We have selected sulfuric acid for this initial study and we find that just above the onset of crystallization, at 0.7 GPa, a previously unobserved monoclinic structure, with $P2_1/c$ symmetry, is formed. As for the low-temperature $C2/c$ phase, the high-pressure crystal structure is also characterised by $SO_2(OH)_2$ tetrahedra interconnected by hydrogen bonds. However, in the high-pressure structure the tetrahedra are no longer arranged in layers but, instead, they form hydrogen-bonded ribbons where the molecules adopt a $R_3^3(12)$ arrangement. A series of *ab initio* calculations indicates that this rearrangement of the molecules results in a relatively small reduction in the enthalpy (13.603 kJ mol^{-1}) for the $P2_1/c$ structure at 0.7 GPa.

Experimental

Crystallography

Liquid sulfuric acid was loaded and pressurised in a Merrill–Bassett diamond-anvil cell[11] that had been equipped with 600 μm culet diamonds and a tungsten gasket. After the nucleation of several crystallites the temperature was cycled close to the melting curve, in order to reduce the number of crystallites, in a manner similar to the methods used by Vos *et al.*[12] Finally, a single crystal was obtained at approximately 0.7 GPa that entirely filled the 200 μm gasket hole.

The diamond-anvil cell was mounted and centred on a Bruker APEX diffractometer (equipped with a monochromated Mo X-ray tube (μ(Mo-Kα) = 0.946 mm^{-1})) and a sequence

Table 1 High-pressure data collection scan sequence for the Bruker APEX CCD diffractometer

Run	2θ/°	ω range/°	ϕ/°	Frames
1	−28.00	−8, −40	90.00	106
2	28.00	40, −40	90.00	266
3	−28.00	−140, −215	90.00	250
4	28.00	−140, −172	90.00	106
5	−28.00	−140, −218	270.00	260
6	28.00	−140, −172	270.00	106
7	−28.00	−8, −40	270.00	106
8	28.00	35, −40	270.00	250

of eight data collection scans was initiated, as detailed in Table 1. The SMART[13] program was used for data collection control and, with a detector distance of 70 mm, 2θ was set at either +28° or −28° to provide maximum coverage while ensuring that the detector surface did not intercept the primary beam. The eight scans were conducted as a sequence of frames that each had a range of 0.3° in ω and had an exposure time of 30 s. The ϕ-axis was fixed at either 90° or 270°, to ensure that the axis of the diamond-anvil cell was held parallel to the $\omega/2\theta$-plane so that absorption from the pressure cell components was minimised and the maximum possible access of reciprocal space could be achieved. As the APEX diffractometer has a three-circle goniometer the χ-axis is permanently fixed at a value of 54.74°. The overall data collection time was 15 h. With the SMART[13] code the sample reflections were identified by hand and an orientation matrix was determined using the GEMINI program.[13] Data integration and global cell refinement were performed with the program SAINT.[13] The monoclinic cell dimensions produced by SAINT for H_2SO_4 were found to be a = 7.695(13), b = 4.559(7), c = 8.378(3) Å, β = 107.42(8)°, V = 280.4(9) Å^3 (T = 293 K) which gives a total of four molecules in the unit cell, on comparison of the unit cell volume of the low-temperature phase.

The program SHADE[10] was used to reject reflections for which either the incident or diffracted beam was completely absorbed by the cell and resulted in the shading of the detector. The data completeness was 36.4%; this low value is a result of the unavoidable shading of reciprocal space by the pressure cell. Although the completeness is substantially lower than would normally be accepted for a typical ambient-pressure study, it is very close to the expected coverage for the design of pressure cell used in the experiment, as will be discussed later. Reflections with very poorly fitting profiles were also rejected. The surviving reflections were corrected for absorption by the pressure cell components with the program SADABS[14] and the transmission ranged from 0.494 to 1.000. The low minimum transmission factor arises due to partial shadowing by the highly absorbing tungsten gasket, which is difficult to model analytically. The structure was solved by direct methods in Pc (SHELXS-97[14]) and subsequently refined against F in $P2_1/c$ symmetry following identification of the crystallographic inversion centres (CRYSTALS[15]). H-atoms were placed on O1 and O2 on the basis of their longer bonds to the sulfur atom and their short intermolecular contacts to O-atoms in neighboring molecules. Chemically equivalent S–O and OSO distances and angles were restrained to be equal. Following refinement of the H-positions in which the OH and SOH distances and angles were restrained to 0.85(1) Å and 109(1)° the H-atom positions were fixed. The S-atom was refined with anisotropic displacement parameters, but the O-atoms were modeled isotropically. A common isotropic thermal parameter was also modeled for the H-atoms. The structure refined to R = 5.99%, R_w = 3.81% for 27 parameters and 178 data with $F > 4\sigma(F)$ and 8 restraints. The final difference map extremes were −0.34 and +0.48 e Å^{-3} and the goodness-of-fit was 1.037. The structural parameters are presented in Table 2 and selected bond lengths and bond angles are listed in Table 3.

CCDC reference number 172536.

See http://www.rsc.org/suppdata/dt/b1/b109395a/ for crystallographic data in CIF or other electronic format.

Theoretical calculations

We have performed *ab initio* calculations that were carried out using the CASTEP code.[16] The calculations were performed within the density functional formalism using a plane wave basis set and also using the generalized gradient approximation[17] that gives an accurate description of the many-body effects of electron exchange and correlation in hydrogen-bonded materials. Vanderbilt ultrasoft pseudopotentials[18] are used to describe the valence electron–ionic core interactions. This is necessary to reduce the size of the basis set in order to make the calculations tractable. The electronic wavefunction is expanded in a plane-wave basis set up to a kinetic energy of 380 eV which we find converges the total energy differences of the system to better than 1 meV atom^{-1}. This required the use of approximately 4×10^6 basis functions. Brillouin zone integrations are performed using a Monkhorst–Pack[19] k-point set. In each of the calculations, a k-point density is chosen such that the total energy of the system is converged to better than 1 meV atom^{-1} in line with the cut-off convergence criteria. The electronic structure is optimised by use of a pre-conditioned conjugate gradients energy minimization scheme. In all cases, the initial geometric configuration was taken from the experimental results, but both the lattice parameters and internal positions have been optimised self-consistently.

We have chosen this *ab initio* method for a number of reasons; a large enough plane wave basis set is guaranteed to be both converged and complete. This is necessary in calculating properties of such complex materials where many different bonding configurations are possible, since *a priori* knowledge of the likely electronic configuration is not available in this case which would be useful in the choice of a localized atomic/molecular orbital basis set. Also, since the basis set is complete, we can make use of the Hellmann–Feynman theorem to calculate forces on the atoms for use in geometric optimization. The positions of the atoms within the unit cell are optimised also using a conjugate gradients method and the *ab initio* forces. Using the *ab initio* methods we find that the lattice parameters are a = 7.905, b = 4.591, c = 8.749 Å and β = 108.17° and the atomic coordinates along with the calculated bond lengths and bond angles are presented in Tables 2 and 3 respectively. We have also performed *ab initio* calculations on the low-temperature structure to make a comparison between the geometries. We find that the relaxed ambient pressure lattice parameters are a = 8.087, b = 5.007, c = 8.899 Å, β = 110.47° and V = 337.58 Å^3, and these compare favorably with the reported experimental values of a = 8.181(2), b = 4.6960(10), c = 8.563(2) Å, β = 110.47° and V = 306.31(12) Å^3. We report the atomic positions in Table 4 and the bond lengths and bond angles in Table 5, where the experimental results of Kemnitz *et al.*[4] have been given for comparison.

For both the high-pressure $P2_1/c$ structure and the low-temperature $C2/c$ structure, the experimentally and theoretically derived bond lengths and bond angles involving the H atoms differ considerably. This is mainly due to the difficulty in obtaining accurate hydrogen positions from X-ray diffraction data. However, the DFT calculations can more accurately determine the hydrogen positions, and consequently the structural parameters involving the hydrogen atoms, and, therefore, it is expected that the results obtained by theory will be more reliable. Furthermore, the PW91 exchange-correlation functional used here is fully *ab initio* (unlike many commonly used functionals in quantum chemistry) and it has been demonstrated that its use in DFT calculations reproduces known hydrogen-bonded structures very accurately (for example references 8, 9 and 10).

Table 2 Fractional coordinates for the high-pressure monoclinic, $P2_1/c$, sulfuric acid structure obtained from the *ab initio* calculations (second set of coordinates) and, for comparison, the coordinates obtained from the Bruker APEX CCD single-crystal X-ray diffraction results. The standard deviations obtained from the single-crystal refinements are shown in parentheses

	Experimental			Theoretical		
Species	*x*	*y*	*z*	*x*	*y*	*z*
S	0.2639(8)	0.0672(9)	0.1787(4)	0.2679	0.0680	0.1840
O(1)	0.0994(17)	−0.111(3)	0.1901(16)	0.1196	−0.1354	0.1958
O(2)	0.316(2)	−0.065(2)	0.0318(12)	0.3348	−0.0625	0.0524
O(3)	0.4062(15)	0.034(2)	0.3289(11)	0.4105	0.0677	0.3344
O(4)	0.199(2)	0.3538(19)	0.1292(13)	0.1861	0.3410	0.1272
H(1)	0.131	−0.289	0.209	0.1432	−0.3500	0.1806
H(2)	0.38	−0.22	0.064	0.4371	−0.2090	0.0952

Table 3 Selected bond lengths (Å) and bond angles (°) for the high-pressure monoclinic, $P2_1/c$, sulfuric acid structure obtained from the single-crystal X-ray diffraction results (first set of numbers) and the *ab initio* calculations. The standard deviations obtained from the single-crystal refinements are shown in parentheses. The symmetry equivalent atomic positions are obtained from: #1 $x, y - 1, z$; #2 $-x + 1, y - 1/2, -z + 1/2$; #3 $-x + 1, y + 1/2, -z + 1/2$; #4 $x, y + 1, z$

	Experimental	Theoretical
S(1)–O(1)	1.537(7)	1.531
S(1)–O(2)	1.537(5)	1.527
S(1)–O(3)	1.416(6)	1.441
S(1)–O(4)	1.407(6)	1.427
O(1)–H(1)	0.85	1.019
O(2)–H(2)	0.85	1.028
O(1)–O(4)#1	2.668(9)	2.571
O(2)–O(3)#2	2.765(11)	2.583
O(3)–H(2)#3	2.05	1.555
O(4)–H(1)#4	1.89	1.564
O(1)–S(1)–O(2)	105.0(4)	105.3
O(1)–S(1)–O(3)	109.3(4)	109.3
O(2)–S(1)–O(3)	110.5(5)	107.9
O(1)–S(1)–O(4)	106.1(5)	106.7
O(2)–S(1)–O(4)	106.8(4)	109.3
O(3)–S(1)–O(4)	118.3(4)	117.3
S(1)–O(1)–H(1)	109	113.5
S(1)–O(2)–H(2)	109	114.0
O(1)–H(1)–O(4)#1	151	177.8
O(2)–H(2)–O(3)#2	142	169.0

Discussion

In the low-temperature phase of sulfuric acid the crystal structure is characterised by layers of $SO_2(OH)_2$ tetrahedra interconnected by hydrogen bonds to form $R_4^4(16)$ nets of molecules. However, the arrangement of the molecules in the $P2_1/c$ phase is strikingly different. At high-pressure the molecules arrange themselves into isolated chains so that the hydrogen-bonding scheme adopts an $R_3^3(12)$ form, see Fig. 1. There are two ribbons running parallel to the *b*-axis, within each unit cell, and the chains are related to one another by the *c*-glide symmetry. The molecules within each ribbon are related by a 2_1 screw axis and they, consequently, form an alternating sequence about the axis. The molecules on either side of the central axis form a pair of strands that are linked together by O1–H ⋯ O4 hydrogen bonds. This arrangement forms a double back-bone of hydrogen bonds which runs along the length of the ribbon. The pair of strands are cross-linked together by O2–H ⋯ O3 hydrogen bonds to complete the box-like form of the full molecular ribbon. The molecular chains are stacked within the crystal so that the edges of the box, as defined by the cross-linking O2–H ⋯ O3 hydrogen bonds, are coplanar and as a consequence layers of ribbons parallel to (1 0 $\bar{2}$) are produced. Inter-layer contacts are formed between O1–O2 (3.08 Å, 3.21 Å), O2–O3 (2.94 Å, 3.15 Å), O3–O3 (2.81 Å) and O2–O2 (3.09) Å while intra-layer contacts are formed between O1–O1 (3.08 Å, 3.25 Å), O1–O2 (3.28 Å) and O1–O4 (3.16 Å).

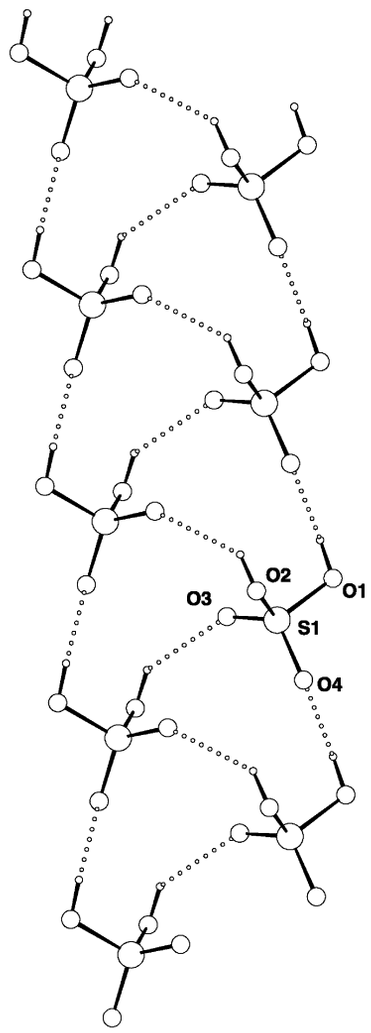

Fig. 1 A view of the molecular chains within the high-pressure monoclinic, $P2_1/c$, crystal structure of sulfuric acid detailing the $R_3^3(12)$ configuration of the hydrogen bonding. The orientation of the figure is approximately along the [0 0 1] direction, with [0 1 0] along the chain direction.

From the *ab initio* pseudo-potential calculations, we find that this arrangement of the molecules in the $P2_1/c$ structure at 0.7 GPa results in a relatively small, 13.603 kJ mol^{-1}, reduction in enthalpy when compared to the arrangement of the molecules in the low-temperature $C2/c$ structure at the same pressure. This reduction in enthalpy is similar in magnitude to our previous calculations on acetic acid (CH_3COOH) and propionic acid (CH_3CH_2COOH) where enthalpy differences of 5.403 kJ mol^{-1} and 5.981 kJ mol^{-1} respectively were found between the low-temperature and high-pressure phases.[9,10] The rearrangement of the H_2SO_4 molecules from the $R_4^4(16)$ hydrogen-bonded layers that characterize the low-temperature structure to the

Table 4 Fractional coordinates for the low-temperature monoclinic, *C*2/*c*, sulfuric acid structure obtained from the *ab initio* calculations (second set of coordinates) and, for comparison, the coordinates obtained from the experimental study of Kemnitz *et al.*[4] The standard deviations obtained from the experimental work are shown in parentheses

	Experimental[4]			Theoretical		
Species	*x*	*y*	*z*	*x*	*y*	*z*
S(1)	0.0000	0.07450(9)	0.2500	0.0000	0.0761	0.2500
O(1)	−0.15928(13)	−0.0822(2)	0.17792(13)	−0.1584	−0.0664	0.1744
O(2)	0.00920(13)	0.2733(2)	0.11080(12)	0.0212	0.2661	0.1203
H(1)	0.088(4)	0.328(5)	0.128(3)	0.1444	0.3411	0.1461

Table 5 Selected bond lengths (Å) and angles (°) for the low-temperature monoclinic, *C*2/*c*, sulfuric acid structure obtained from the experimental studies of Kemnitz *et al.*[4] (first set of values) and, for comparison, the numbers obtained from the *ab initio* calculations. The standard deviations obtained from the single crystal refinements are shown in parentheses. The symmetry equivalent atomic postions are obtained from: #1 $-x, y, -z + 1/2$, #2 $x + 1/2, y + 1/2, z$

	Experimental[4]	Theoretical
S(1)–O(1)	1.426(1)	1.427
S(1)–O(2)	1.537(1)	1.533
O(2)–H(1)	0.66(3)	1.018
O(1)#2–H(1)	1.99(3)	1.570
O(1)#2–O(2)	2.648(2)	2.367
O(1)#2–H(1)–O(2)	170.0(3)	155.7
O(1)–S(1)–O(1)#1	117.87	116.9
O(2)–S(1)–O(2)#1	105.22	105.8
O(1)#1–S(1)–O(2)	110.70	110.7
O(1)–S(1)–O(2)	105.85	106.1

$R_3^3(12)$ form of the chains found in the high-pressure structure is accompanied by a more efficient molecular packing: in the low-temperature structure, at 113 K, each molecule occupies a volume of 76.58 Å^3 while at high-pressure the molecular volume is 69.85 Å^3. This 9% reduction in molecular volume is significantly greater than those observed in either acetic acid or propionic acid where the volume decrease between the low-temperature and high-pressure phases was only 3% and 2% respectively.

Finally, we have performed a Mulliken population analysis on the systems, which allows us to examine the nature of the charge transfer between the various species in the structures which gives a qualitative description of the relative strengths of the hydrogen bonds. The methods described in references 20 and 21 were used to calculate the Mulliken charges on each of the atoms, but it is worth noting that several other methods exist and therefore the actual values of the charges can vary from method to method. They should not, therefore, be taken as the actual atomic charge, which in any case, is rather ambiguously defined. However it is generally thought that the direction of charge transfer will be correct. We find that in both the *C*2/*c* phase and the $P2_1/c$ phase at ambient pressure and at 0.74 GPa the atomic charges are the same in each case; the charge on S atoms is 2.55 e, O is −0.91 e and H is 0.54 e. It therefore appears that the molecular charge distribution is relatively insensitive to the environment of the molecules (at least at these relatively low pressures). As pressure is increased from ambient to 0.74 GPa the intra-molecular bond lengths and angles remain relatively unchanged and, as is expected, it is mainly the inter-molecular separations that decrease. A comparison of the intra-molecular S–O bond lengths and O–S–O bond angles in Tables 3 and 5 indicates that they are essentially the same between the *C*2/*c* and $P2_1/c$ phases, with a retention of the long ($P2_1/c$: S(1)–O(1), S(1)–O(2); *C*2/*c*: S(1)–O(2)) and short ($P2_1/c$: S(1)–O(3), S(1)–O(4); *C*2/*c*: S(1)–O(1)) bonds. Hence, the molecular properties remain similar over the pressure range investigated. Therefore, the charge on the atoms forming the hydrogen bond remains the same for the low-temperature and high-pressure structures indicating that they have very similar strengths. This is also indicated by the low enthalpy difference between the two structures given that the molecular shapes are very similar.

In conclusion, we have solved the high-pressure monoclinic $P2_1/c$ structure of sulfuric acid and find that this previously unobserved phase has a radically different hydrogen bonding topology to that observed in the low-temperature *C*2/*c* phase. The high-pressure structure is composed of molecular ribbons adopting an $R_3^3(12)$ hydrogen bond scheme whereas the low-temperature phase is formed from $R_4^4(16)$ layers of molecules. This rearrangement not only offers a marked improvement in molecular packing efficiency but also results in a modest reduction of the enthalpy.

The present study is a further development in the use of area detectors for high-pressure single-crystal X-ray diffraction that we implemented in our recent work on the high-pressure phase of propionic acid. In this initial study, we used a conventional four-circle Eulerian goniometer (Bruker P4) equipped with the Bruker SMART 1000 CCD detector and sets of ω-scans were performed at 30° intervals in χ. The completeness of the resulting data set was 29%. The combination of the Bruker P4 and a CCD detector is somewhat non-standard and, conventionally, Bruker CCD detectors are used in conjunction with three-circle goniometers. Although the scan range is much more limited than in the four-circle instrument, we find that the use of a three-circle machine does not reduce the completeness of the resulting high-pressure data sets and a completeness of 36.4% is produced—which is somewhat better than that obtained with the four-circle goniometer and is close to the maximum 40% volume of reciprocal space that it is possible to access with a diamond-anvil cell of the Merrill–Bassett design. This is a significant consideration as our results indicate that it is possible to collect an almost ideal high-pressure data set from a CCD diffractometer that has neither its mechanical design nor its data collection control software modified for the purpose. Apart from the application of the SHADE program after data integration and the use of a short collimator, high-pressure data collection and refinement follow a relatively standard procedure that can be easily implemented at any X-ray laboratory equipped with a CCD machine. As CCD goniometers are now in wide use and are increasingly supplanting point-detector diffractometers, it can be anticipated that high-pressure studies will be performed by a greater number of workers at non-specialized laboratories.

Acknowledgements

This work is supported by a grant from the Engineering and Physical Sciences Research Council (EPSRC) of the United Kingdom. P. A. McGregor and A. Dawson also express gratitude to the EPSRC for their Ph.D. studentships.

References

1 W. F. Giaque, E. W. Hornung, J. E. Kunzler and T. R. Rubin, *J. Am. Chem. Soc.*, 1960, **82**, 62.
2 J. Kendall and E. Brakeley, *J. Am. Chem. Soc.*, 1921, **43**, 1826.

3 B. P.-G. Jönsson and I. Olovsson, *Acta Crystallogr., Sect. B*, 1968, **24**, 559.
4 E. Kemnitz, C. Werner and S. Trojanov, *Acta Crystallogr., Sect. C*, 1996, **52**, 2665.
5 A. R. Moodenbaugh, J. E. Hartt, J. J. Hurst, R. W. Youngblood, D. E. Cox and B. C. Frazer, *Phys. Rev. B*, 1983, **28**, 3501.
6 R. J. Nelmes, *Ferroelectrics*, 1987, **71**, 87.
7 R. J. Nelmes, Z. Tun and W. F. Kuhs, *Ferroelectrics*, 1987, **71**, 125.
8 D. R. Allan and S. J. Clark, *Phys. Rev. Lett.*, 1999, **82**, 3464.
9 D. R. Allan and S. J. Clark, *Phys. Rev. B*, 1999, **60**, 6328.
10 D. R. Allan, S. J. Clark, S. Parsons and M. Ruf, *J. Phys.: Condens. Matter*, 2000, **12**, L613.
11 L. Merrill and W. A. Bassett, *Rev. Sci. Instrum.*, 1974, **45**, 290.
12 (*a*) W. L. Vos, L. W. Finger and R. J. Hemley, *Nature*, 1992, **358**, 46; (*b*) W. L. Vos, L. W. Finger and R. J. Hemley, *Phys. Rev. Lett.*, 1993, **71**, 3150.
13 R. A. Sparks, GEMINI, Bruker AXS, Madison, Wisconsin, 1999; R. A. Sparks, SMART, Area-Detector Software Package, Bruker AXS, Madison, Wisconsin, 1993; R. A. Sparks, SAINT, Area-Detector Software Package, Bruker AXS, Madison, Wisconsin, 1995.
14 G. M. Sheldrick, SADABS, A Program for Empirical Absorption Correction of Area Detector Data, University of Göttingen, Germany, 1996; G. M. Sheldrick, SHELXS-97, University of Göttingen, Germany, 1997.
15 D. J. Watkin, C. K. Prout, J. R. Carruthers, P. W. Betteridge and R. I. Cooper, CRYSTALS, Issue 11, Chemical Crystallography Laboratory, Oxford, UK, 2001.
16 M. C. Payne, M. P. Teter, D. C. Allen, T. A. Arias and J. D. Joannopolous, *Rev. Mod. Phys.*, 1992, **64**, 1045.
17 J. P. Perdew and Y. Wang, *Phys. Rev. B*, 1992, **46**, 6671.
18 D. Vanderbilt, *Phys. Rev. B*, 1990, **41**, 7892.
19 H. J. Monkhorst and J. D. Pack, *Phys. Rev. B*, 1976, **13**, 5188.
20 M. D. Segal, R. Shah, C. J. Pickard and M. C. Payne, *Phys. Rev. B*, 1996, **54**, 16317.
21 M. D. Segal, R. Shah, C. J. Pickard and M. C. Payne, *Mol. Phys.*, 1996, **89**, 571.